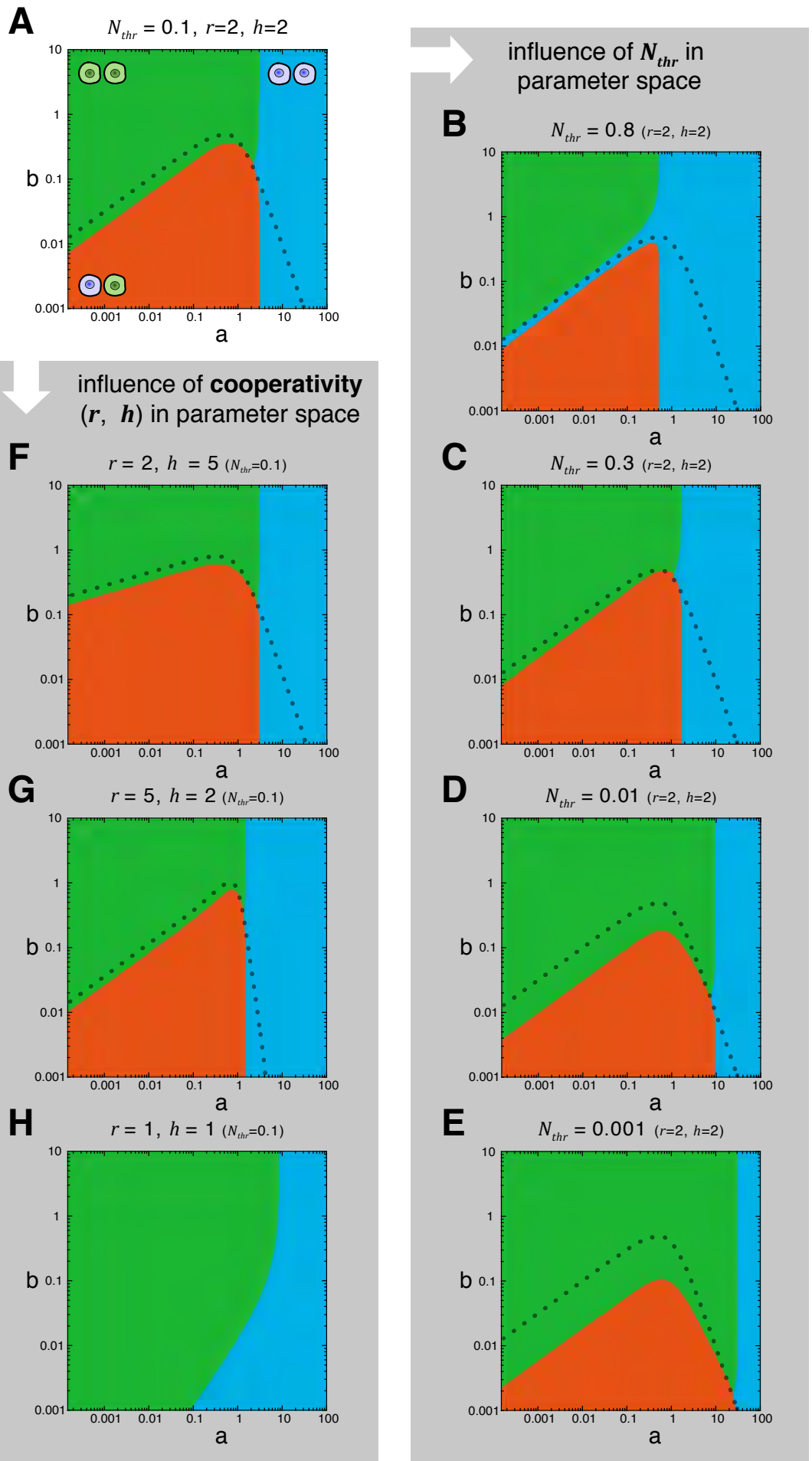
A
N_{thr} = 0.1, r=2, h=2
influence of N_{thr} in parameter space
B
N_{thr} = 0.8 (r=2, h=2)
C
N_{thr} = 0.3 (r=2, h=2)
D
N_{thr} = 0.01 (r=2, h=2)
E
N_{thr} = 0.001 (r=2, h=2)
influence of cooperativity (r, h) in parameter space
F
r = 2, h = 5 (N_{thr}=0.1)
G
r = 5, h = 2 (N_{thr}=0.1)
H
r = 1, h = 1 (N_{thr}=0.1)
a
b
10
1
0.1
0.01
0.001
0.001
0.01
0.1
1
10
100

Supplementary Figure S1. The model behaviour is robust to variations in N_{thr} and cooperativity strength. **A**. Fate profiles in parameter space as in Fig. 2A, for comparison. **B-E**. Phase space for N_{thr} equal to 0.8 (B), 0.3 (C), 0.01 (D), and 0.001 (E), respectively (with $r, h = 2$ in all cases). The dotted line marks the stability boundary for the 'homogeneous' solutions (pairs of identical cells), and serves as reference for comparison with (A). While in B (where $N_{thr} > 0.7$), the area of asymmetric fate is surrounded by symmetric negative resolution, in C-E the organisation of the phase space is very similar to A, with the transitions shifting along the stability boundary. **F-H**. Phase space when cooperativity is either increased (in the repression of Dl by activated N, with $h = 5$, in F; or in the activation of N by Dl, with $r = 5$, in G) or eliminated (with $r, h = 1$, in H). ($N_{thr} = 0.1$ in all cases). Phase space in F, G is qualitatively similar to A, but not in H, where the asymmetric pairs are lost.

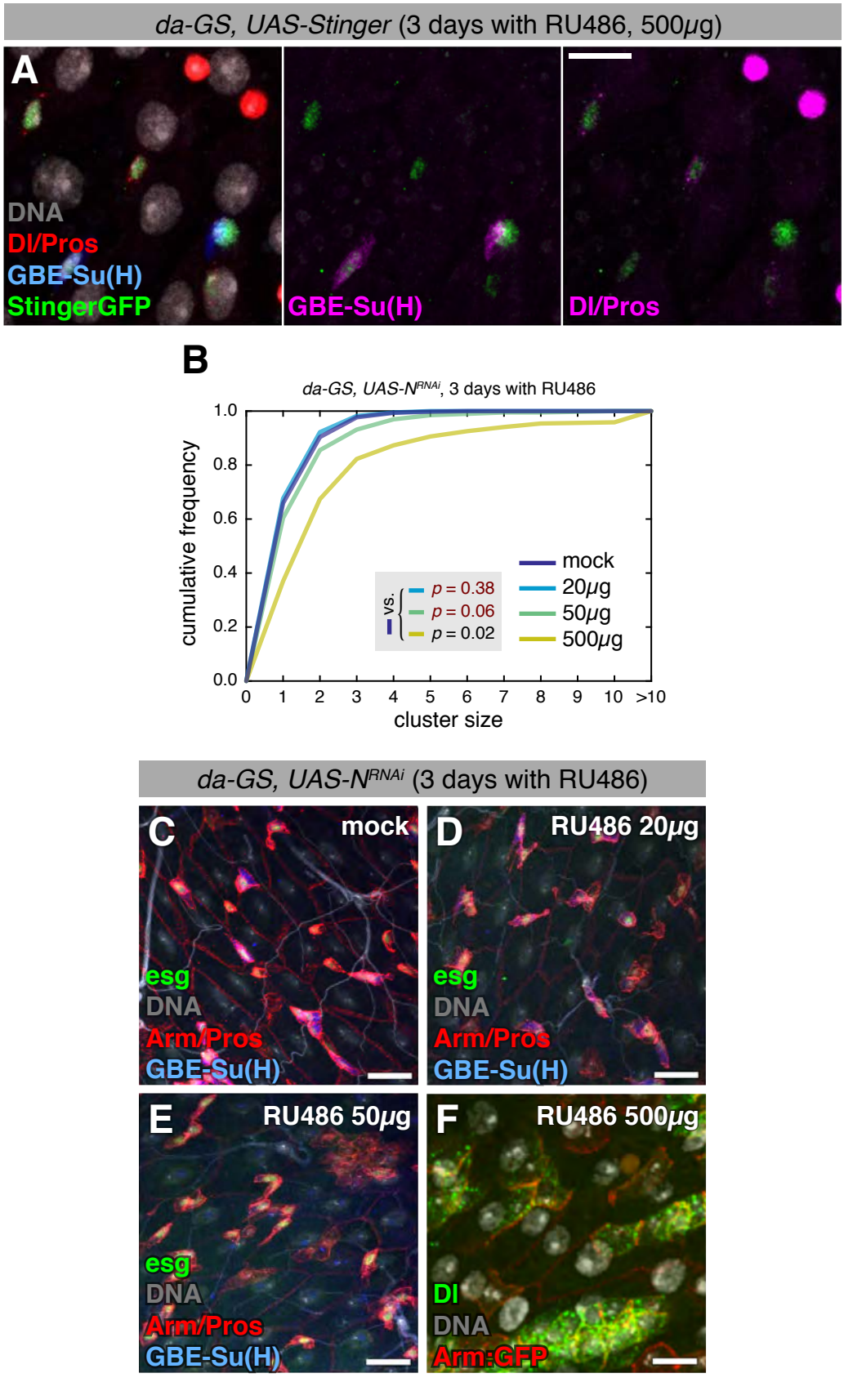

Supplementary Figure S2. *Notch* knock-down using *da-GS* is EB and ISC-specific and can induce a phenotypic series. **A**. Confocal micrograph showing the expression pattern of the *da-GS* driver, shown with *UAS-Stinger*. The same panel is repeated three times: left, with all markers (Stinger, green; Delta/Prospero, red; *GBE-Su(H)-lacZ*, blue; DNA, grey), center, with Stinger and *GBE-Su(H)-lacZ* (purple) only, and right, with Stinger and Delta/Prospero (purple) only. Delta accumulates at the membrane and vesicles; Prospero is nuclear. Note expression is highly specific of ISCs (Delta^{+}) and EBs (*GBE-Su(H)-lacZ*$^{+}$), only occasionally showing expression in EEs (Pros^{+}; not shown). **B.** Cumulative frequency of nest size for *da-GS, UAS-N*^{RNAi} flies with different RU486 treatments, with N = {956, 782, 394, 457} for mock, 20, 50 and 500*μ*g/vial, respectively. Note the similarity in distributions between mock, 20 and 50*μ*g/vial (with only the latter having a barely significant p-value), which breaks down evidently with 500*μ*g/vial. **C-F.** Confocal micrographs showing esg^{+} cell nests after mock treatment (C) and *Notch* knock-down induced with 20 (D), 50 (E) and 500*μ*g/vial (F), respectively. ISC-like tumours are starting to form only with the 500*μ*g/vial treatment.

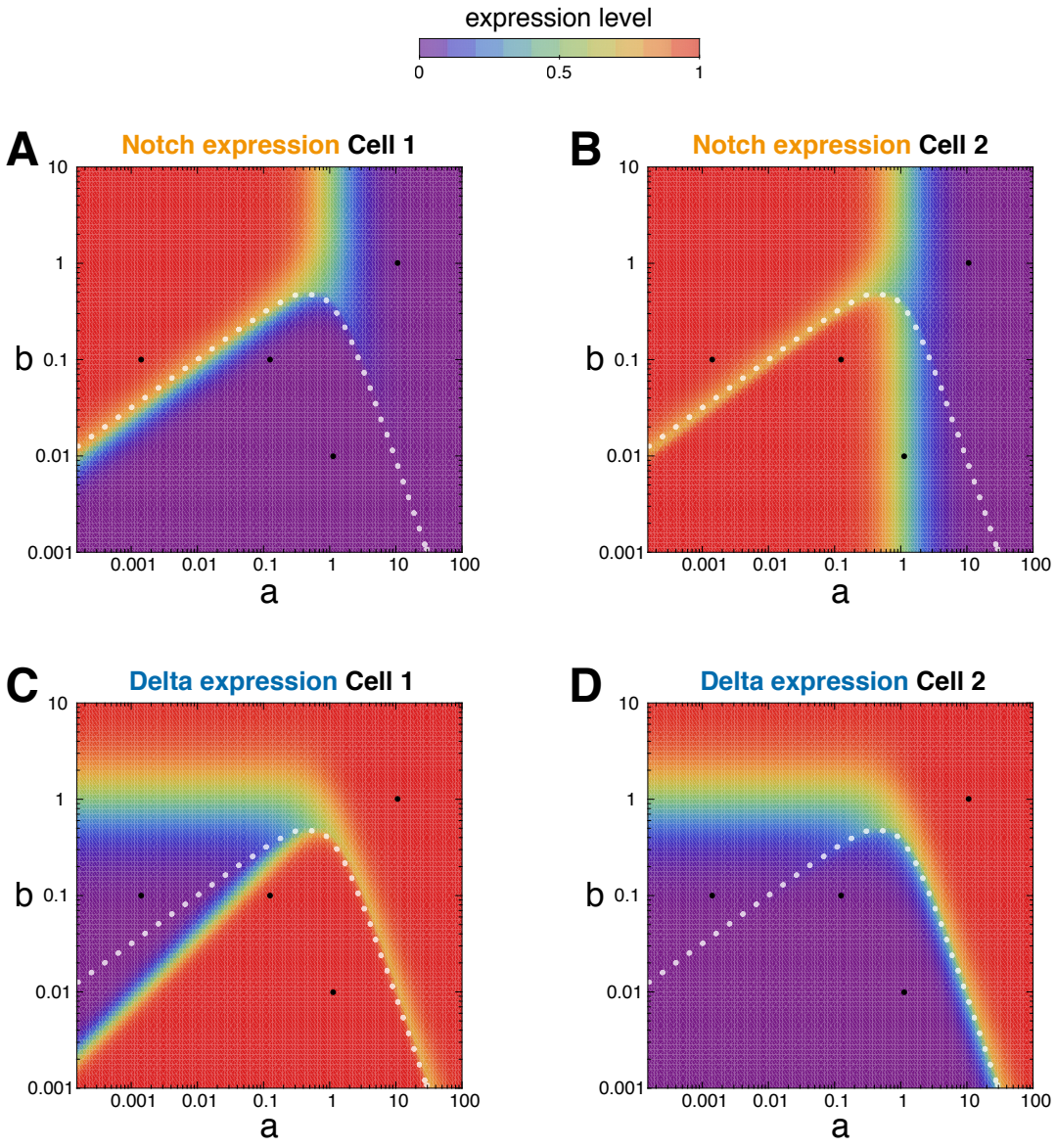

Supplementary Figure S3. Values of Notch and Delta at steady state across parameter space for $r = 2, h = 2$ (as in Figure 2A). Dotted line, boundary of stability for steady states with identical cells. The black dots mark the parameter values used in (Collier et al., 1996) (Figure 2B) and the asymmetric, symmetric positive and symmetric negative pairs from Figure 2C-E. **A, B.** Steady-state values of activated Notch in the two cells of a pair (one in each panel) respect to a, b. **C-D.** Steady-state values of Delta in the two cells of a pair (one in each panel) respect to a, b. Note that depending on the value of activated Notch, one can find symmetric negative or symmetric positive fate profiles below the boundary (region of heterogeneous solution), showing that the model allows for symmetric steady states where cells in a pair do not have identical amounts of Notch or Delta.

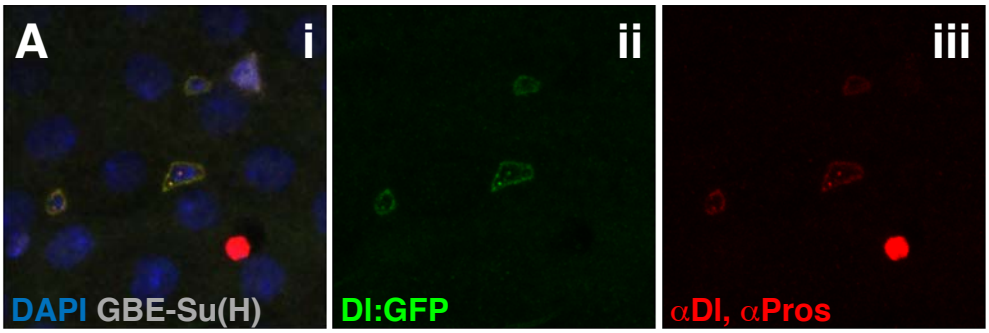

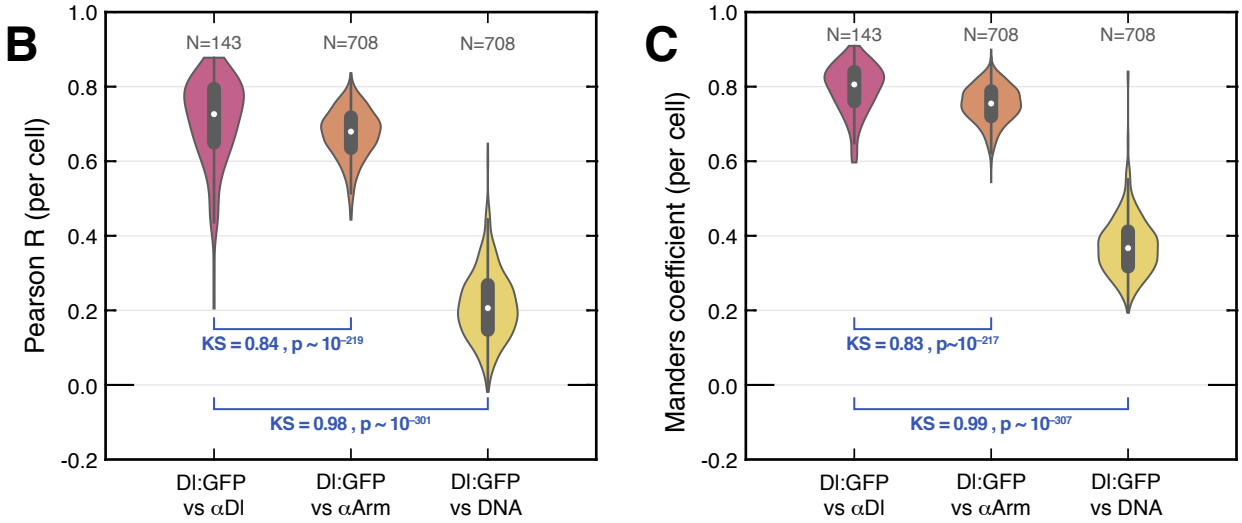

Supplementary Figure S4. Co-localisation between immunodetection of Delta and GFP using *Delta*$^{MI04868\text{-}GFSTF.1}$. **A.** Confocal micrograph illustrating the co-localisation of anti-Dl and anti-GFP in *Delta*$^{MI04868\text{-}GFSTF.1}$*/+* intestines. (Image shows the projection of several confocal planes). **B-C**. Co-localisation measurements between anti-Dl, anti-GFP (for *Delta*$^{MI04868\text{-}GFSTF.1}$), anti-Arm as a general membrane marker and Hoechst to label DNA, taken in 3D stacks for individual cells. N indicates the number of cells measured per experiment. Considering either Pearson correlation coefficient (B) or Manders co-localisation coefficient (C), the data show a high level of co-localisation between anti-Dl and anti-GFP, with very significantly higher coefficient values than between anti-GFP and Hoechst (which would give the baseline values for anti-correlation in this setting) as well as between anti-GFP and anti-Arm. The latter comparison indicates that the level of correlation between anti-Dl and anti-GFP cannot be from just coinciding randomly in the membrane and demonstrates that, at this level of spatial resolution, detection of *Delta*$^{MI04868\text{-}GFSTF.1}$ with anti-GFP is a very good indicator of the spatial distribution of Delta.

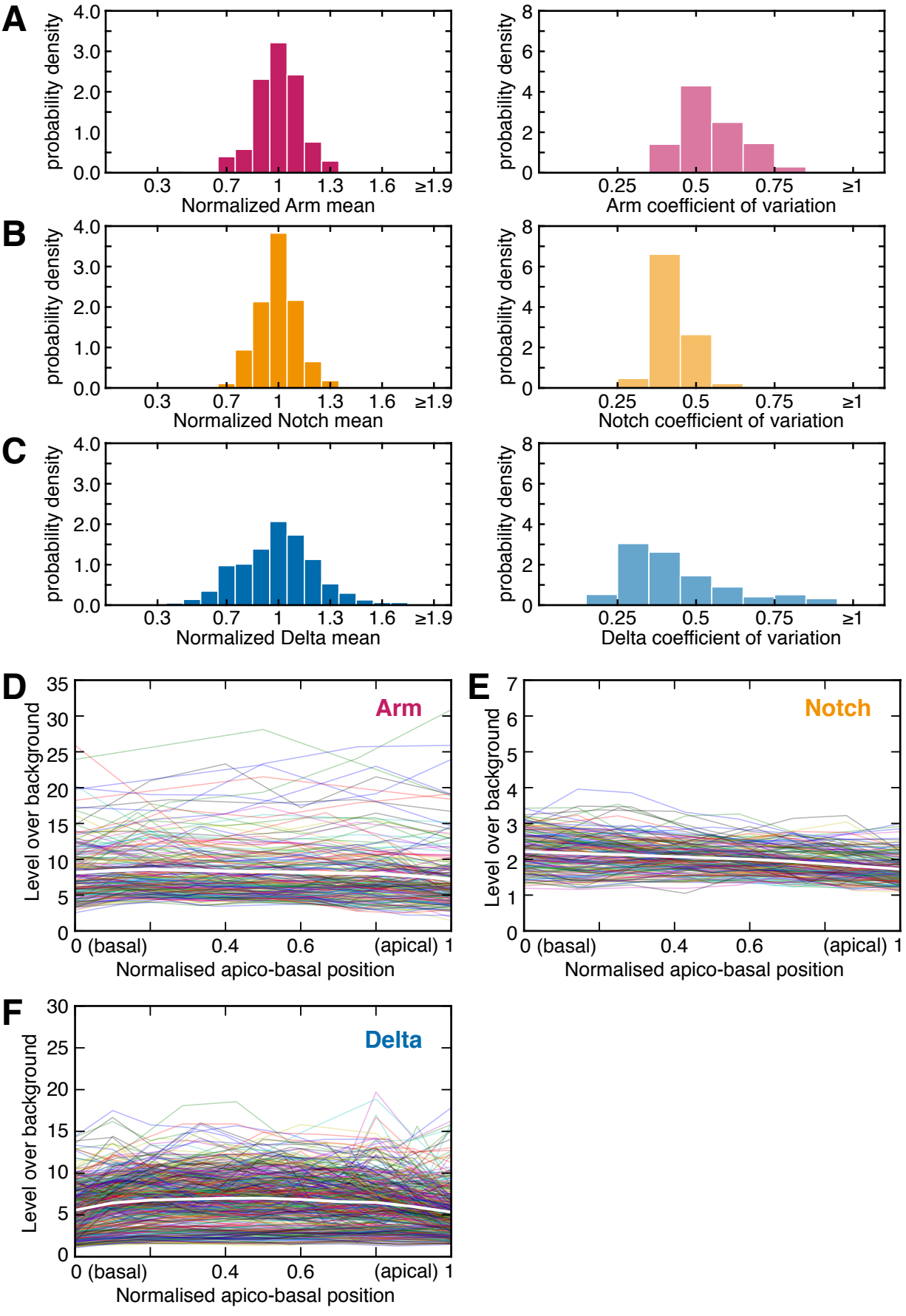

Supplementary Figure S5. Distribution of Arm, Notch and Delta at the membrane. **A-C.** Histograms of the normalised mean intensity per plane (left hand panels) and the coefficient of variation (CV) per plane (right hand panels) for Arm (A), Notch (B) and Delta (C). The normalised mean intensity in plane *i* is defined as the ratio of the average of the plane and the average for the cell. Data correspond to 46 cells (single and paired) for Notch and Armadillo, and 66 cells (paired) for Delta. **D-F**. Distribution of Arm (D), Notch (E) and Dl (F) levels along the apical-basal cell axis (with height of the cell normalised to 1). Each cell contributes ten lines to the plot, corresponding to the intensity values along the vertical axis of non-overlapping, angular windows of 2π/10. Data displayed in D-E are from 20 paired esg+ cells and data in F are from 43 cells.

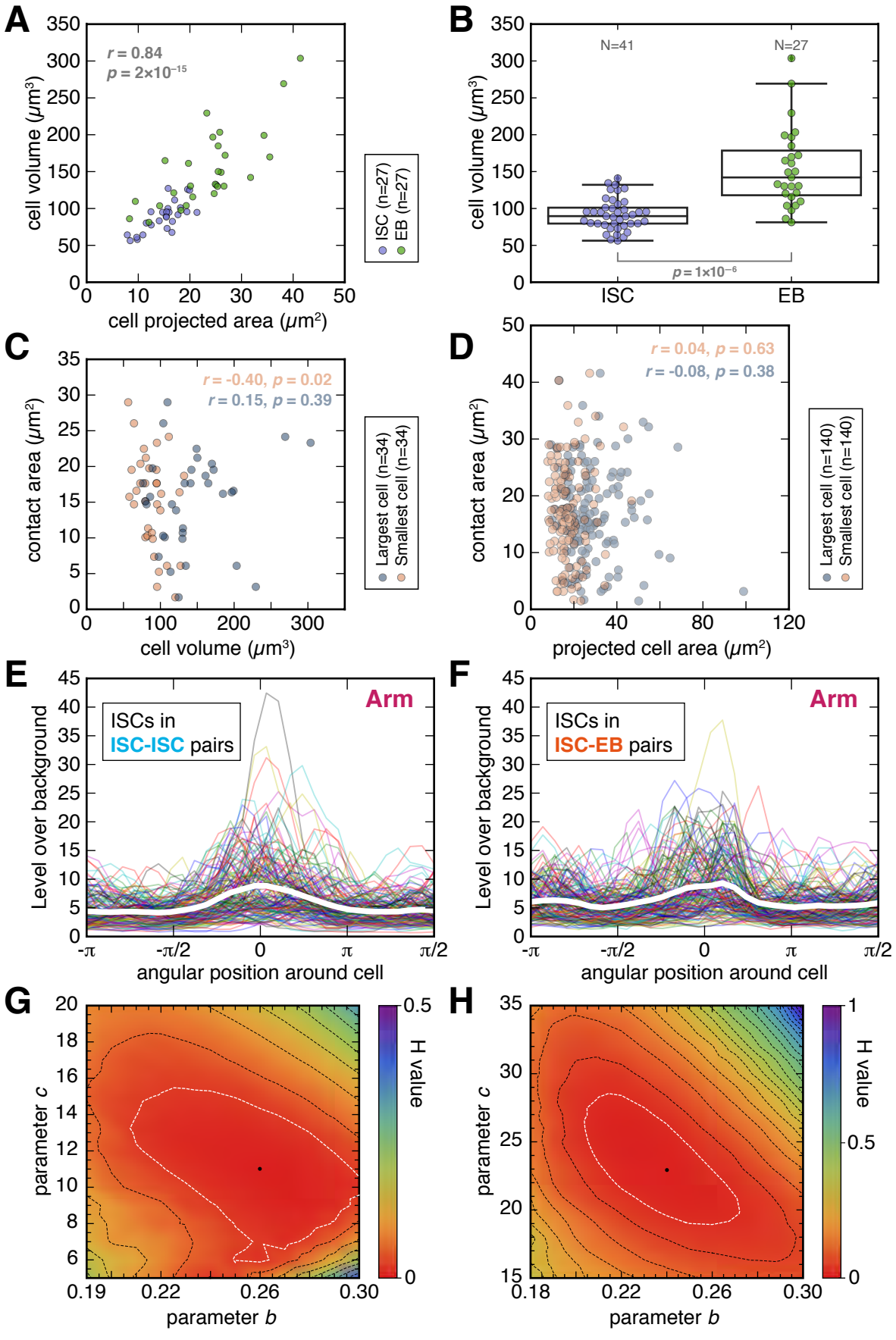

Supplementary Figure S6. Relationships between cell size, Arm levels and contact area, and statistical comparison between theoretical and experimental pair frequencies. Data in A-D are from the cell set from Figure 4B. **A**. Correlation between cell volume and projected cell area for EBs and ISCs, showing that projected area is a good predictor of total volume. **B**. Comparison of volume between ISCs and EBs. EBs are ~60% larger, with statistical significance. **C**. Correlation between contact area and projected cell area of the cells in the pair. The larger cells in each pair (usually an EB) is represented in dark blue and the smaller (usually an ISC) in light brown. **D**. Correlation between cell volume and projected cell area of the cells in the pair. Colour scheme is as in C. **E-F**. Arm levels along the perimeter of ISCs in either ISC-ISC (E) or ISC-EB (F) pairs, for all cells confocal planes (colour lines), with the mean value (white). For each cell plane, position 0 corresponds to the centre of the contacting membranes (defined as the position that intersects the line connecting the cell centroids in that plane). Data in E-F are from 20 ISC-EB and 23 ISC-ISC pairs. **G-H**. Kullback-Leibler relative entropy (*H*) between experimental and model distributions of *Notch* wild-type (G) or mock *Notch* knockdown (H) cell pair frequencies as a function of *b* and *c* (note the difference in scale between the two parameters). Values of area in the model are generated by the SKD depicted in Fig. 4C. Best fits (black dots) correspond to $b = 0.26$, $c = 11$ (G) and $b = 0.24$, $c = 23$ (H). Black discontinuous lines mark isovalues every 0.05 *H* units. White discontinuous lines enclose the area for $H \leq 0.02$; the upper and lower limits of *b* in these areas define the height of the boxes in the parameter space indicated in Fig. 4G.